

# Effect of Crystallite Size on the Thickness of Nonmagnetic Shell and Magnetic Properties of $\text{La}_{0.7}\text{Ca}_{0.3}\text{MnO}_3$

Thi Anh Ho · Tran Dang Thanh · The-Long Phan ·  
Suhk Kun Oh · Seong-Cho Yu

Received: 9 June 2014 / Accepted: 29 August 2014 / Published online: 19 September 2014  
© Springer Science+Business Media New York 2014

**Abstract**  $\text{La}_{0.7}\text{Ca}_{0.3}\text{MnO}_3$  compounds with the crystallite size of  $D = 45\text{--}200$  nm were synthesized by utilizing the solid-state reaction and mechanical ball milling methods. The reduction of the crystallite size ( $D$ ) resulted in the decrease of both  $T_C$  and magnetization, broadening of the phase transition region, and appearance of Griffiths phase features in the materials. The temperature dependence of saturation magnetization ( $M_S$ ), the variations of the coercivity ( $H_C$ ), and the deviation of magnetization from expected Bloch's law  $T^{3/2}$  for these samples were also investigated. Based on the core-shell model, the core diameter and the nonmagnetic shell thickness for the samples were determined.

**Keywords** Nanocrystals · Perovskite manganites · Magnetic properties · Core/shell-like structure

## 1 Introduction

Recently, the effect of crystallite size reduction on the physical properties of hole-doped manganites has attracted lots of interest of scientists for both fundamental and application aspects [1–5]. Owing to finite-size effect and inter-particle interactions, remarkable new phenomena were

observed in nano-materials [1]. The inter-particle interaction was found to be strongly modifying the magnetic response of nanoparticle systems; e.g., the dc susceptibility obeys the Curie-Weiss law rather than the Curie law at high temperatures. Moreover, the magnetic behavior of the particle surface differs from that of the core [2, 3]. Higher magnetic disorder that is usually present in the surface layer is known as a dead magnetic layer. Before one investigates the magnetic behavior of manganites in nanoscales, one has to prepare nanomaterials through a variety of synthesis methods. However, almost authors have used the bottom-up approach (e.g., sol-gel, mechanochemical milling, interactive milling, or sputtering methods) to prepare nanostructured samples. In this work, instead, we have used a simple preparative method that is the top-down approach to prepare nano-polycrystalline  $\text{La}_{0.7}\text{Ca}_{0.3}\text{MnO}_3$  (LCMO) samples and have investigated their magnetic properties.

## 2 Experiment

First, LCMO ceramic samples were prepared by conventional solid-state reaction. High-purity powders  $\text{La}_2\text{O}_3$ ,  $\text{CaCO}_3$ , and Mn were used as starting materials. These powders were ground and mixed well, and then heated in air at  $1,200^\circ\text{C}$  for 24 h. After heating, the obtained powder was re-ground, pressed into pellets, and sintered at  $1,400^\circ\text{C}$  for 24 h in air. These pellets were then used for mechanical ball milling (by using a Spex 8000D system) with the mass ratio of ball/powder = 4.1/1. The milling time ( $t_m$ ) was varied from 0 to 30 min (denoted as LC0, LC10, LC20, and LC30 for  $t_m = 0, 10, 20,$  and 30 min, respectively). Their structure was checked by using an X-ray diffractometer (Siemens D5000, with  $\lambda = 1.5406 \text{ \AA}$ ). The surface morphology of samples has been observed by

T. A. Ho · T.-L. Phan · S. K. Oh · S.-C. Yu (✉)  
Department of Physics, Chungbuk National University, Cheongju,  
361-763, South Korea  
e-mail: scyu@chungbuk.ac.kr

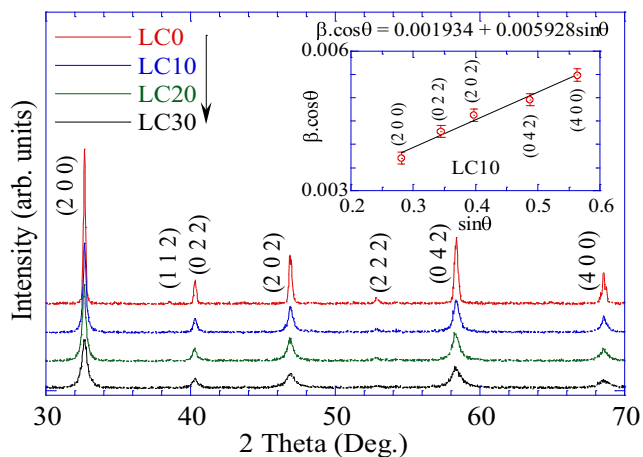
T. D. Thanh (✉)  
Institute of Materials Science, Vietnam Academy of Science and  
Technology, 18-Hoang Quoc Viet, Hanoi, Vietnam  
e-mail: thanhxraylab@yahoo.com

scanning electron microscopy (SEM). The  $M(T)$  and  $M(H)$  curves were measured via a SQUID magnetometer.

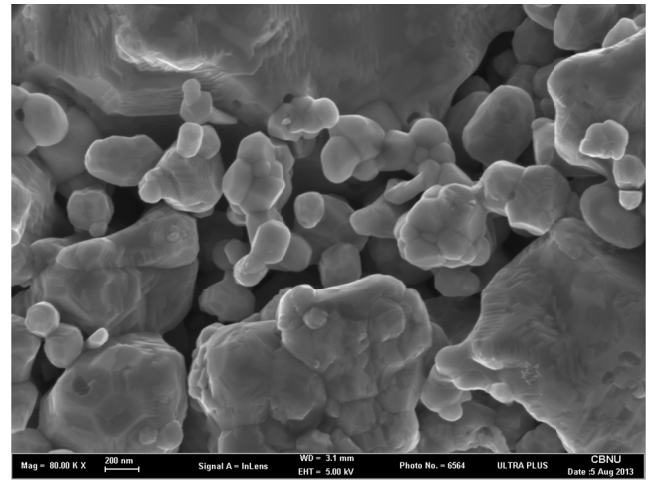
### 3 Results and Discussions

Figure 1 shows the X-ray diffraction (XRD) patterns for the LCMO samples with various  $t_m$  values. Our detailed analyses, i.e., identifying the Miller-indexed peaks, reveal that they are single phase in an orthorhombic structure, with the lattice parameters  $a \approx 5.48 \text{ \AA}$ ,  $b \approx 7.75 \text{ \AA}$ , and  $c \approx 5.46 \text{ \AA}$ . The lattice parameters were almost independent of  $t_m$ . Using the Williamson-Hall (W-H) method [6], the average values of both the crystallite size ( $D$ ) and strain ( $\varepsilon$ ) parameters could be obtained from the relation  $\beta \cos \theta = (K\lambda / D) + 2\varepsilon \sin \theta$  where  $\beta$  is the full width at a half maximum of an XRD peak,  $\theta$  is the Bragg angle, and  $K = 0.9$  is the shape factor. The W-H analysis for LC10 is representatively shown in the inset of Fig. 1. The crystallite size obtained for  $t_m = 0, 10, 20,$  and  $30$  min are  $D = 200, 72, 54,$  and  $45$  nm, and  $\varepsilon = 0.002, 0.003, 0.003,$  and  $0.010$ , respectively. Notably,  $D = 200$  nm is herein an estimated value for the as-prepared sample ( $t_m = 0$ ), and its real value can be larger because the W-H method is more accurate for the size of nanoparticles smaller than  $100$  nm. Figure 2 shows the SEM image for a representatively sample, LC10. In comparison with the SEM image, the  $D$  values deduced from W-H method are in good agreement.

Figure 3a shows the temperature dependence of field-cooled (FC) and zero-field-cooled (ZFC) magnetizations of the samples in the field of  $H = 100$  Oe. The  $T_C$  values determined from the minima of the  $dM/dT$  vs.  $T$  curves are  $252, 252, 248,$  and  $246$  K for  $D = 200, 72, 54,$  and  $45$  nm, respectively. Here, the reduction in  $D$  did not change the  $T_C$  significantly, but it broadened the phase transition region.



**Fig. 1** XRD patterns for LCMO samples. The inset shows a detailed W-H analysis for the LC10 sample



**Fig. 2** SEM image for LC10 sample

The width of the FM-PM phase transition ( $\Delta T_C$ ) determined from the full width at half maximum of the  $dM/dT$  vs.  $T$  curve increases from  $6$  to  $34$  K with decreasing  $D$  from  $200$  to  $45$  nm. In Fig. 3b, we showed the  $\chi^{-1}(T)$  curves deduced from  $M_{ZFC}(T)$  data. One can see that in the high-temperature region,  $\chi^{-1}$  varies almost linearly with temperature following the Curie-Weiss law [7],  $\chi(T) = C/(T - \theta)$ , where  $C$  is the Curie constant, and  $\theta$  is the ordering temperature. Here,  $\theta$  decreases gradually in the temperature range of  $251$ – $240$  K with decreasing  $D$ . This confirms that the strength of FM interaction decreases in LCMO nanoparticles with a smaller crystallite size. Notably,  $\chi^{-1}(T)$  data at high-temperature regions obey the Curie-Weiss law well for LC0 sample with  $D = 200$  nm, whereas for samples with smaller crystallite sizes ( $D = 72, 54,$  and  $45$  nm), the Curie-Weiss law is not satisfied in the full PM temperature range. That is because there are obviously sharp downturns in  $\chi^{-1}(T)$  curves well above  $T_C$ , which is the characteristic of the Griffiths singularity [8]. It means that the Griffiths phase exists in LCMO nanoparticles. This could be explained by higher degree of disorder in nanoparticle

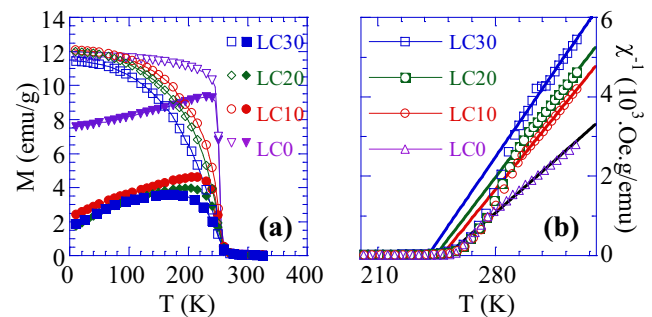


**Fig. 3** a ZFC (solid symbols) and FC (open symbols)  $M(T)$  curves with  $H = 100$  Oe. b  $\chi^{-1}(T)$  data fitted to the Curie-Weiss law (solid lines)

samples than that in as-prepared sample (LC0). According to Salamon et al. [8], the disorder due to the bending of Mn-O-Mn bond induces the formation of Griffiths phase in the  $\text{La}_{1-x}\text{Ca}_x\text{MnO}_3$  system.

Figure 4a shows hysteresis loops of  $M(H)$  curves measured at 5 K. One can see that the magnetization value was reduced in the smaller LCMO nanoparticles. This reduction is related to the nonmagnetic layer or spin disorder on the surface; its thickness increases with decreasing  $D$ . The coercivity ( $H_C$ ) value substantially increases when the crystallite size decreases see the inset in Fig. 4a. A monotonic decrease of  $H_C$  with increasing temperature in the range of 5–240 K becomes more rapid when temperature increases above 240 K see Fig. 4b. This is associated with the FM-PM phase transition, where magnetic moments located within FM domains/clusters become disordered due to thermal agitation. At temperatures above  $T_C$ , the value of  $H_C$  is thus almost 0, in good agreement with the above  $M(T)$  analyses. Interestingly, the  $H_C$  observed below  $T_C$  increases with decreasing  $D$ . The  $H_C$  at 5 K as a function of the surface/volume ratio ( $D^{-1}$ ) is shown in the inset of Fig. 4b. In general, when  $D$  is reduced,  $H_C$  increases and reaches a maximum value at some critical diameter ( $D_{cr}$ ) of the single domain state, and then, it decreases with further decrease in the crystallite size [7]. The solid line in the inset of Fig. 4b is a fit of our experimental  $H_C$  data to the function  $H_C = m + n/D$ , where  $m$  and  $n$  are constants [7]. This indicates that our LCMO systems are close to a multidomain structure [9]. It means that the  $D$  values are larger than  $D_{cr}$  values of the single domain state, which makes the anisotropy energy smaller. Hence, the  $H_C$  value decreases monotonically with increasing  $D$  as shown in the inset of Fig. 4b.

We have also determined the saturation magnetization ( $M_S$ ) for the samples at different temperatures. From  $M^2(H)$  curves, the linear extrapolation from high fields to the intercepts with the  $M^2$ -axis gives the values of

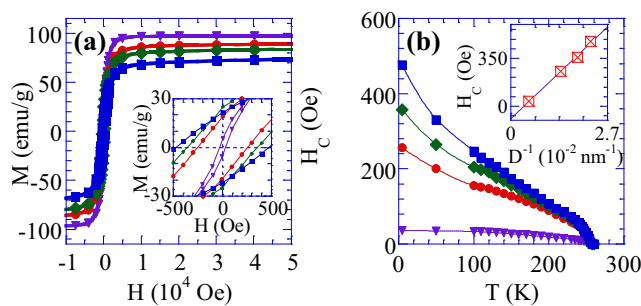


**Fig. 4** **a**  $M$  vs.  $H$  measured at 5 K. The inset shows the zoom-in view of the region between  $H = -500$  and  $500$  Oe. **b**  $H_C$  as a function of  $T$ . The inset shows  $D^{-1}$  dependence of  $H_C$  at 5 K. Here, triangles, circles, diamonds, and squares indicate LC0, LC10, LC20, and LC30 samples, respectively

$M_S^2(T, 0)$ . The obtained  $M_S(T)$  data are plotted in Fig. 5a. A power law form of  $M_S(T) = M_S(0)[1 - BT^\epsilon]$  [7] is used to fit the data with  $M_S(0) = 97.0, 86.4, 78.9,$  and  $68.6$  emu/g,  $B = 1.46 \times 10^{-6}, 4.05 \times 10^{-4}, 3.17 \times 10^{-3},$  and  $7.30 \times 10^{-3} \text{ K}^{-\epsilon}$ ; and  $\epsilon = 3.07, 2.13, 1.77,$  and  $1.61$  for  $D = 200, 72, 54,$  and  $45$  nm, respectively. One can see that the temperature dependence of the magnetization do not follow Bloch’s law, but obeys a  $T^\epsilon$  law with  $\epsilon$  increasing from 1.61 to 3.07 when  $D$  increases from 45 to 200 nm (see the solid lines in Fig. 5a). The variation tendency of the exponent  $\epsilon$  for our samples is quite similar to a previous report [10]. Additionally, the  $M_S(0)$  value obtained is smaller than that of the LCMO bulk single crystal ( $M_S(0) = 97.5$  emu/g) [11]. The  $M_S(0)$  values for the samples are reduced linearly with  $D^{-1}$  (see Fig. 5b). This result is consistent with that reported by Lopez-Quintela et al. [12], confirming that the magnetization is actually influenced by the particle surface. We used a model of the core-shell structure [13] to determine the core diameter ( $d_C$ ) for magnetic particles in the samples. The LCMO particles are assumed to have a spherical shape, and each of them is composed of an ideal single-crystalline core with the saturation magnetization of the core,  $M_C = 97.5$  emu/g [11], and the density of  $\rho_C = 5.9 \text{ g/cm}^3$  [14]. For a particle of radius  $r$ , consisting of a core surrounded by a shell of thickness  $d_{\text{shell}} \ll r$  (with the corresponding  $\rho_S$  value roughly assigned to be  $4 \text{ g/cm}^3$  [3]), the core diameter ( $d_C$ ) can be found from [13]

$$d_C = D \cdot \left[ \frac{\rho_S/\rho_C}{\rho_S/\rho_C + (M_C - M_S)/(M_S - M_{\text{Shell}})} \right]^{\frac{1}{3}} \quad (1)$$

By using (1), while assuming a nonmagnetic shell ( $M_{\text{Shell}} = 0$ ), the  $d_C$  values obtained are 199.5, 67.9, 48.9, and 38.3 nm for  $D = 200, 72, 54,$  and  $45$  nm, respectively. Clearly, the nonmagnetic shell thickness, which can be estimated by  $d_{\text{shell}} = (D - d_C)/2$ , increases from 0.25 to 3.35 nm with decreasing  $D$ . The increase in  $d_{\text{shell}}$  and decrease in  $D$  (or the increase in  $D^{-1}$ ) are the main reason for the reduction in the strength of FM inter-particle

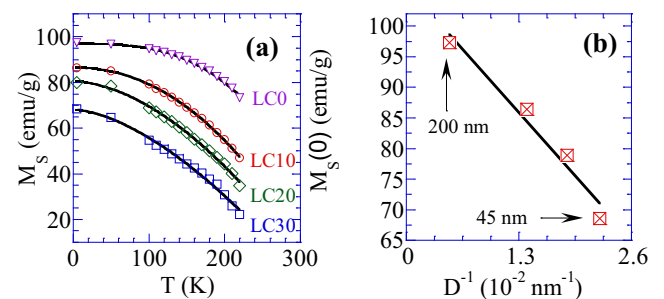


**Fig. 5** **a**  $M_S$  vs.  $T$  for the samples (symbols) is fitted to a power law  $T^\epsilon$  (solid lines). **b**  $D^{-1}$  dependence of  $M_S(0)$

interactions and in the  $M_S$  for LCMO nanoparticles, as mentioned above.

#### 4 Conclusion

The analyses of the magnetic properties were performed for LCMO nanoparticles with the crystallite size of  $D = 45$ – $200$  nm. Based on  $\chi^{-1}(T)$  curves, the existence of Griffiths phase in LCMO nanoparticles was observed, which implied the higher degree of disorder in nanoparticle samples. The results show that the  $D$  values of our LCMO samples are larger than the  $D_{cr}$  of the single domain state. Therefore,  $H_C$  value increases monotonically with decreasing  $D$ . Also, the temperature dependence of magnetization in this case obeys a power law  $T^\varepsilon$ , with  $\varepsilon > 3/2$ . The reduction in  $M_S$  vs.  $D$  is mainly due to the formation of a nonmagnetic surface shell surrounding the nanoparticles, which increases from  $0.25$  to  $3.35$  nm when  $D$  is decreased from  $200$  to  $45$  nm.

**Acknowledgments** This research was supported by the Converging Research Center Program through the Ministry of Science, ICT and Future Planning, South Korea (2014048835), and by the National Foundation for Science and Technology Development (NAFOSTED) under grant number 103.02-2012.57 in Vietnam. Some measurements were performed on facilities belonging to the National Key Laboratory for Electronic and Devices, Institute of Materials Science, VAST, Vietnam.

#### References

- Majestich, S.A., Sachan, M.J.: Magnetostatic interactions in magnetic nanoparticle assemblies: Energy, time and length scales. *Phys. D Appl. Phys.* **39**, R407 (2006)
- Dey, P., Nath, T.K., Manna, P.K., Yusuf, S.M.: Enhanced grain surface effect on magnetic properties of nanometric  $\text{La}_{0.7}\text{Ca}_{0.3}\text{MnO}_3$  manganite: Evidence of surface spin freezing of manganite nanoparticles. *J. Appl. Phys.* **104**, 103907 (2008)
- Manh, D.H., Phong, P.T., Thanh, T.D., Nam, D.N.H., Hong, L.V., Phuc, N.X.: Size effects and interactions in  $\text{La}_{0.7}\text{Ca}_{0.3}\text{MnO}_3$  nanoparticles. *J. Alloys Compd.* **509**, 1373 (2011)
- Marin, L., Morellon, L., Algarabel, P.A., Rodriguez, L.A., Magen, C., Teresa, J.M.D., Ibarra, M.R.: Enhanced magnetotransport in nanopatterned manganite nanowires. *Nano. Lett.* **14**, 423 (2014)
- Liang, Y.C., Zhong, H., Liao, W.K.: Nanoscale crystal imperfection-induced characterization changes of manganite nanolayers with various crystallographic textures. *Nanoscale Res. Lett.* **8**, 345 (2013)
- Williamson, G.K., Hall, W.H.: X-ray line broadening from filed Al and W. *Acta Metall.* **1**, 22 (1953)
- Kittel, C. *Introduction to Solid State Physics*, 7th edn, p. 423. Wiley, New York (2000)
- Salamon, M.B., Lin, P., Chun, S.H.: Colossal magnetoresistance is a griffiths singularity. *Phys. Rev. Lett.* **88**, 197203 (2002)
- Curiale, J., Sanchez, R.D., Troiani, H.E., Ramos, C.A., Pastoriza, H., Leyva, A.G., Levy, P.: Magnetism of manganite nanotubes constituted by assembled nanoparticles. *Phys. Rev. B* **75**, 224410 (2007)
- Xi, S., Lu, W., Sun, Y.: Magnetic properties and magnetocaloric effect of  $\text{La}_{0.8}\text{Ca}_{0.2}\text{MnO}_3$  nanoparticles tuned by particle size. *J. Appl. Phys.* **111**, 063922 (2012)
- Song, H., Kim, W., Kwon, S.J.: Magnetic and electronic properties of transition-metal-substituted perovskite manganites- $\text{La}_{0.7}\text{Ca}_{0.3}\text{Mn}_{0.95}\text{X}_{0.05}\text{O}_3$ . *J. Appl. Phys.* **89**, 3398 (2001)
- Lopez-Quintela, M.A., Hueso, L.E., Rivas, J., Rivadulla, F.: Intergranular magnetoresistance in nanomanganites. *Nanotechnology* **14**, 212 (2003)
- Gangopadhyay, S., Hadjipanayis, G.C., Dale, B., Sorensen, C.M., Klabunde, K.J., Papaefthymiou, V.: Magnetic properties of ultra-fine iron particles. *Phys. Rev. B* **45**, 9778 (1992)
- Alwi, H.A., Abd-Shukor: Thermal diffusivity and related properties of colossal magnetoresistive  $\text{La}_{0.67}\text{Ca}_{0.33}\text{MnO}_3$  with various grain sizes. *IEEE Trans. Magn.* **45**, 2899 (2009)